SUPPORTING INFORMATION

Development of a united atom force field for TFB

TFB oligomers are modeled with a united atoms force field (ff). The ff is based on the AMBER parameterization [77] (AMBER united atom [78] for alkyl chains) and is complemented with quantum chemical calculations for atomic charges, torsional potentials and small adjustments of equilibrium values of bond distances and angles.
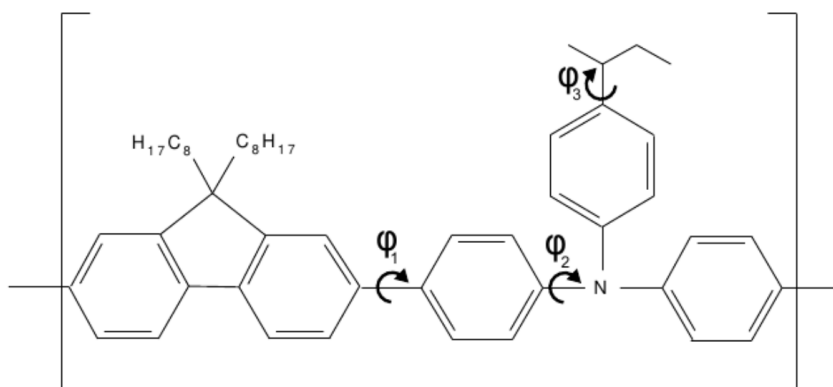

FIG. S1. Repeat unit of the TFB copolymer with indication of the three re-parameterized dihedrals.

Atomic charges are calculated for a model oligomer composed of 4 fluorene-triphenylamine repeat units, terminated with a fluorene moiety, and with alkyl chains substituted by hydrogen atoms. The optimized structure is consistent with the AM1-optimized tetramer reported in ref. [27], showing planar fluorene blocks and a fluorene-triphenylamine dihedral angle (φ_1 in fig. S1) of 36 degrees. The triphenylamine block presents coplanar central NCCC atoms and a propeller-like arrangement of phenyl rigs with a CNCC dihedral angle (φ_2 in fig. S1) of 40 degrees [37, 79]. Atomic charges were calculated on the optimized structure with the electrostatic potential (ESP) fitting method from B3LYP/cc-pVDZ calculations. The reproduction of the molecular dipole moment was imposed in the fit. The geometry optimization and the calculation of ESP charges are performed with the Gaussian09 code [80].

Our ff describes TFB as a sequence of chemically bounded identical units, with all fluorene and triphenylamine co-monomers having the same atomic charges. In order to obtain the set of atomic charges, atoms of co-monomers were labelled as shown in the upper panel of figure S2 and the charge on each atom type was averaged over the central co-monomers of the

oligomer (4 fluorenes, 3 triphenylamines), excluding the terminal units. The bottom panels of figure S2 show ESP charges (red crosses) and the average charge (black squares) for each atom type of fluorene (left) and triphenylamine (right). The average value is representative for the charge of each atom type and it is therefore used as a good approximation for the simulation of oligomers or polymers. United atoms of fluorene octyl chains, corresponding to aliphatic CH, CH_2, and CH_3 groups, are assumed to be electrically neutral.
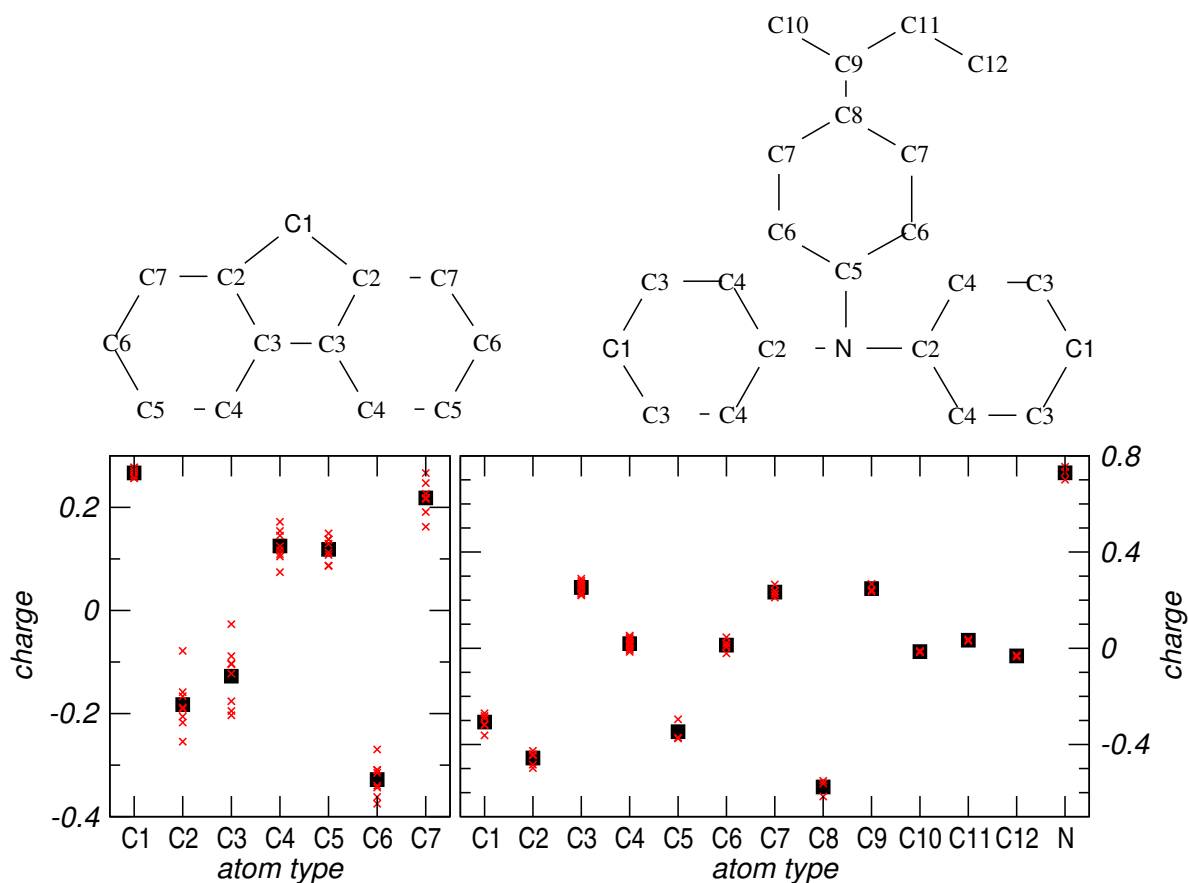

FIG. S2. Top: Definition of charge-atom types for the two TFB co-monomers FLU (left) and TPA (right). Bottom: ESP charges on the central co-monomers of each atom types (red crosses) and respective average values (black squares).

Torsional disorder along polymer chains is very important since it is expected to affect the localization of excess charges on polymer segments. The torsional potentials associated with the three dihedrals sketched in figure S1 are here accurately parameterized from DFT calculations. Quantum mechanical torsional potentials, calculated with relaxed geometry scans of the relevant dihedral angle at the B3LYP/6-31G** level of theory, are plotted with

black squares (and red circles for φ_2) in figure S3. Note that the φ_2 potential depends on the scanning direction as already reported in the literature [37, 79]. This dependence on the scanning direction results from the steric hindrance among phenyl rings arranged in a propeller-like fashion.

The DFT torsional potential is then introduced in the ff following a well-established procedure described in previous works [81] and shortly summarized here. The torsional potential of the ff is the sum of an explicit dihedral potential plus an implicit contribution from other interactions in the ff, i.e. $U_{ff}(\phi) = U_{Dih}(\phi) + U_i(\phi)$. To introduce the quantum-mechanical potential in the ff, we first measured the implicit potential, $U_i(\phi)$, from a separate simulation with $U_{Dih}(\phi)$ set to 0, performed on a fluorene-triphenylamine-fluorene molecule with an inert gas to facilitate energy redistribution trough the sample (40 Ar atoms in a cubic box of side 50 Å). Classical free-energy torsional potentials are computed with adaptive biasing force (ABF) simulations [82] performed at a temperature of 400 K. Once $U_i(\phi)$ is known, the explicit dihedral potential, $U_{Dih}(\phi)$, is obtained by fitting the difference between the DFT potential and $U_i(\phi)$ with a series of cosines. The final ff parameters are reported in table S1. The reparametrized ff torsional potentials, shown as green lines in figure ??, closely reproduce the DFT ones. The oligomer geometries optimized with the ff and at the DFT level are consistent within an accuracy of 0.005 Å for bond lengths, 3 degrees for bending angles and 5 degrees for dihedral angles.

TABLE S1. Force field parameters for dihedral potential of the three torsions in figure S1, expressed as a cosine expansion $U_{Dih}(\phi) = \sum_n k_n[1 + \cos(n\phi - \phi_n^0)]$. Force constants and angles are expressed in kcal/mol and degrees, respectively.

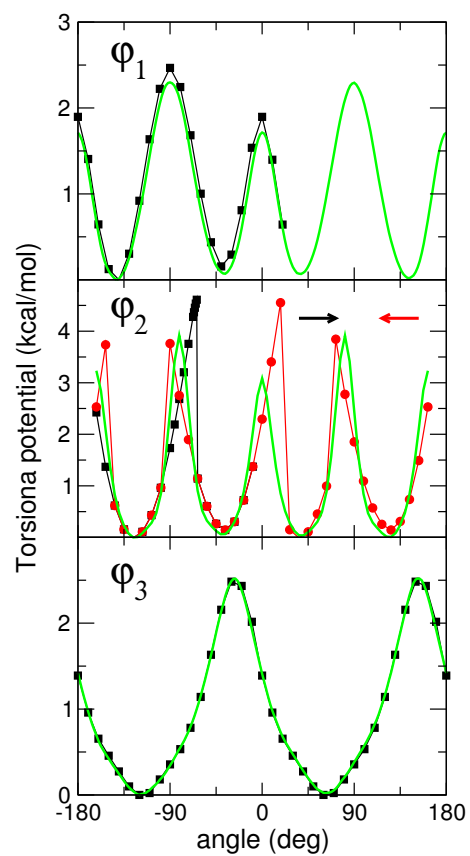|	φ_1			φ_2			φ_3	
n	k_n	ϕ_n^0	n	k_n	ϕ_n^0	n	k_n	ϕ_n^0
2	0.958	180	2	1.843	180	2	1.259	-129.2
4	0.243	0	4	0.235	0	4	0.476	-138.6
6	0.057	0	6	0.101	180	6	0.203	-155.9
8	0.024	0	8	0.197	0			

FIG. S3. Torsional potential for the three dihedrals defined in figure S1 calculated at different level: Black squares report the potential obtained with B3LYP/6-311G** relaxed scans (for φ_2 red circles correspond to a relaxed scan performed in the opposite direction direction, see arrows). Green lines show the ff torsional potential, black and red lines are a guide for the eye.
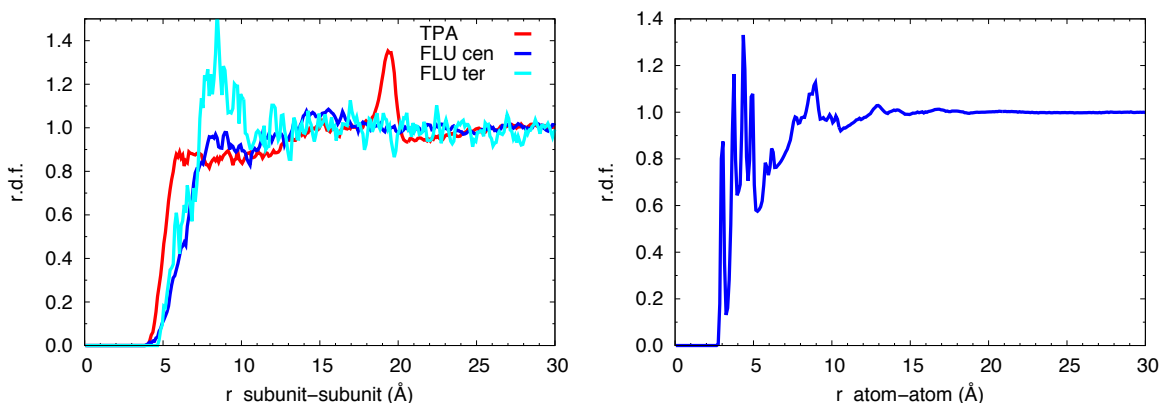
ADDITIONAL TABLES AND FIGURES

FIG. S4. Left: Radial distribution functions calculated between centers of mass of triphenylamine and fluorene subunits. The curves reveal the absence of crystalline order in the sample, with the sharp peak at about 19 Å for TPA corresponding to units belonging to the same oligomer. Right: Radial distribution function between aromatic carbons (with implicit hydrogen, i.e. CH united-atom). Occasional π-stacking between the aromatic rings, revealed by the scattered peaks between 3 and 4 Å, is present but not prevalent. Again the peak at 10 Å originates from an intra-chain correlation.
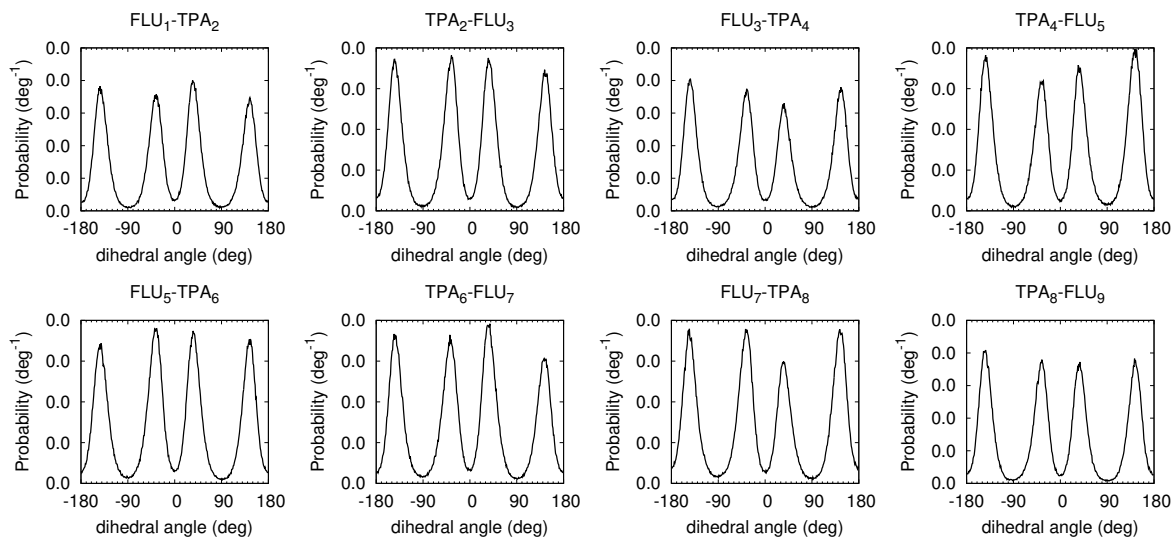

FIG. S5. Distribution of fluorene-triphenylamine dihedral angles along the oligomer chain, indicating that the prevalent conformation is not planar, and consequently the conjugation length for charged oligomers turns out to be very short (two units).

TABLE S2. Hole reorganization energies (λ in meV) for TFB oligomers, calculated with the four point method[34] with ORCA 3.0[83]. In these calculations, octyl and butyl alkyl chains replaced with hydrogen atoms.

method	TFB_1	TFB_2	TFB_3	TFB_4	TFB_5
PBE//DZ	0.146	0.091	0.056	0.043	0.034
B3LYP//6-31G*	0.177	0.116	0.113	0.052	0.021
PBE0//6-31G	0.214	0.143	0.112	0.057	0.023
PBE0//6-31G*	0.218	0.150	0.109	0.070	0.024
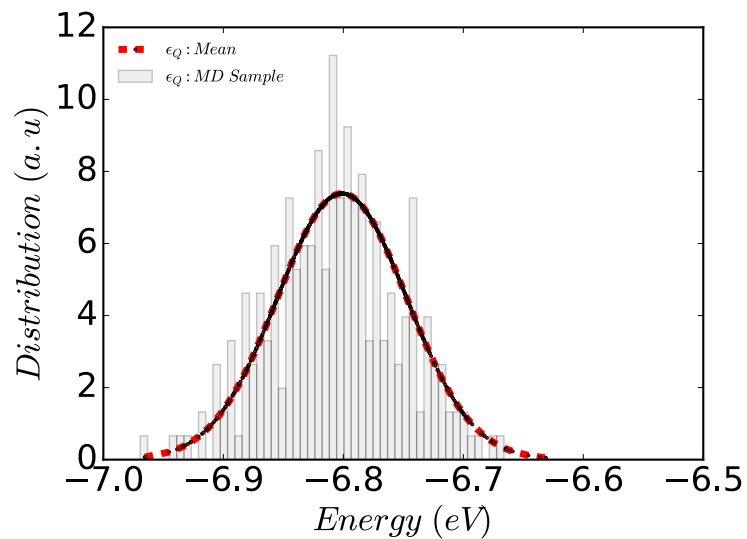
FIG. S6. Distribution of ZINDO site energies of the four MD samples and corresponding Gaussian fit with a standard deviation σ_ϵ=50.2 meV.
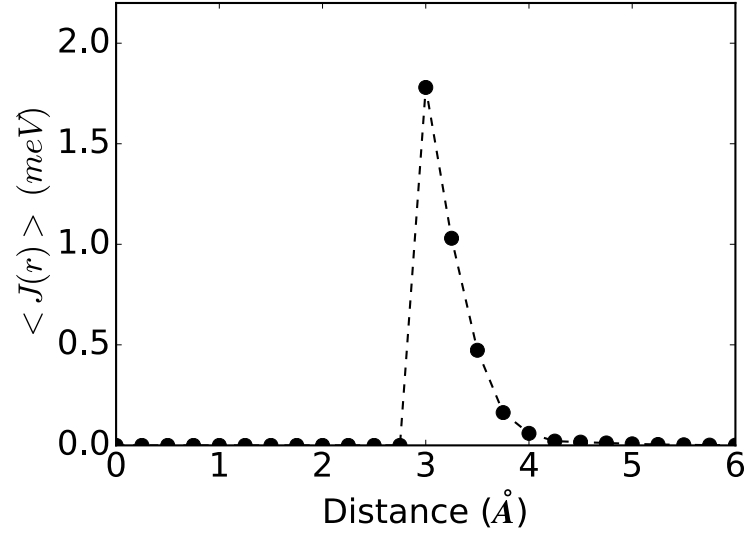
FIG. S7. Average transfer integral as a function of the minimum interatomic carbon-carbon distance between atoms belonging to different oligomers. The rapid decay with distance is well reproduced by an exponential function $J_0 e^{-d/d_0}$ with $J_0 = 6.05$ eV and $d_0 = 0.37$ Å.
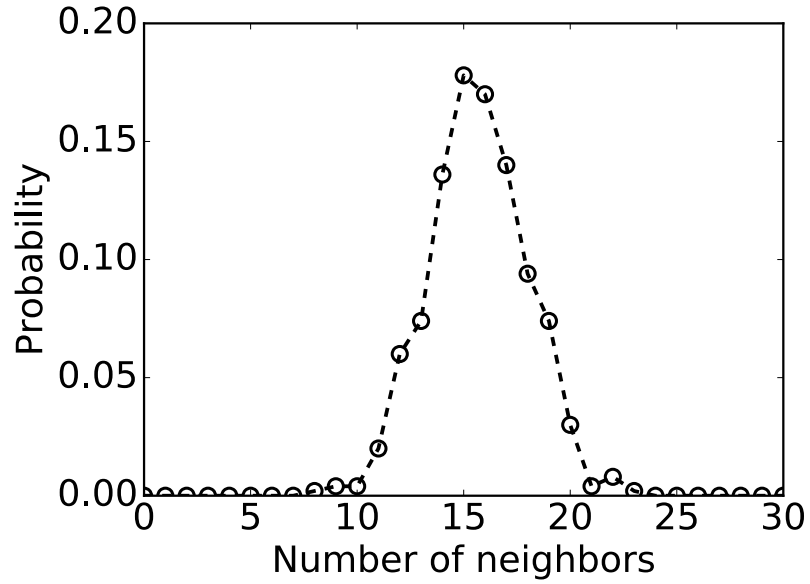

FIG. S8. Distribution of number of neighbors per TFB oligomer in MD samples, calculated using an intermolecular atom–atom cutoff of 6 Å and including only contacts with transfer integral greater than 0.1 meV.
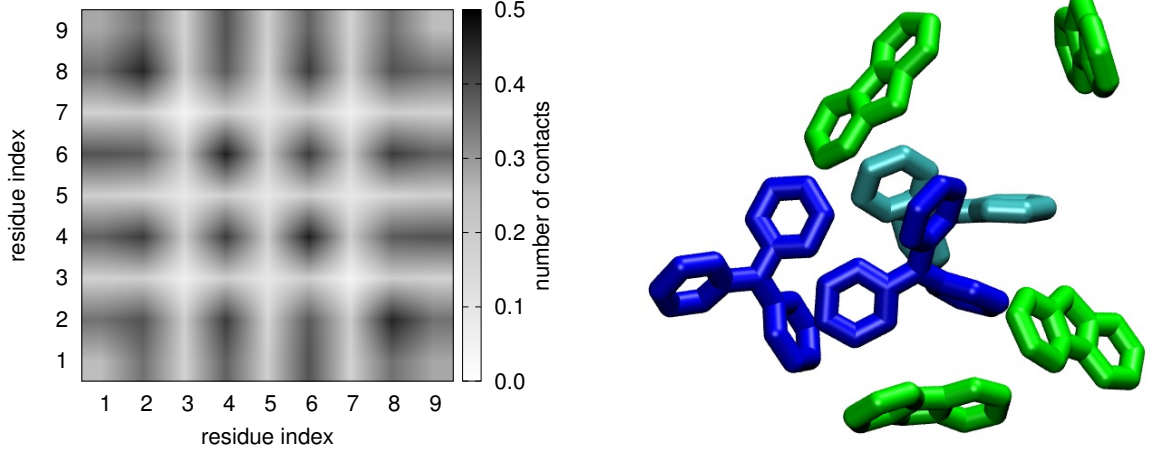
FIG. S9. Left: distribution of the number of neighbors with transfer integral greater than 0.1 meV along the TFB oligomer chain. Odd and even numbers (residue index in the figure axes) correspond to fluorene and triphenylamine units, respectively. Right: example of the neighbours of a central TPA unit (cyan, carbon-carbon cutoff of 6 Å) (TPA in blue, FLU in green). The only π-stacking like contact is with the TPA at the center. The maximum coupling for the whole oligomer to which the central TPA belongs to, is 1.6 meV.
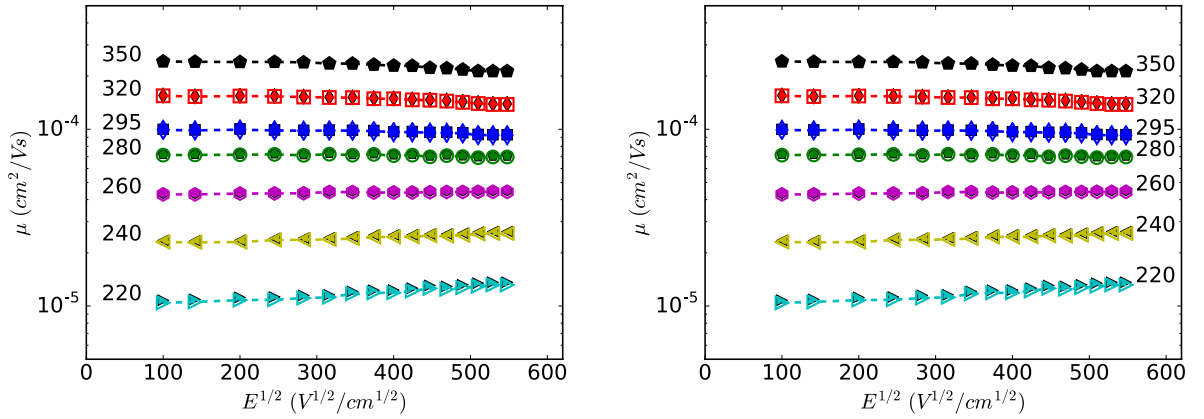

FIG. S10. Simulated mobility of replicated samples as a function of electric field, with site energies randomized at the beginning of each KMC run with σ=50.2 meV and fixed transfer integrals. Left: 2 by 2 replicas of the MD samples ($R^2|\epsilon_G^S|J_Q$); right: 3 by 3 replicas ($R^3|\epsilon_G^S|J_Q$). Points correspond to arithmetic averages, dashed lines to logarithmic averages of mobility.
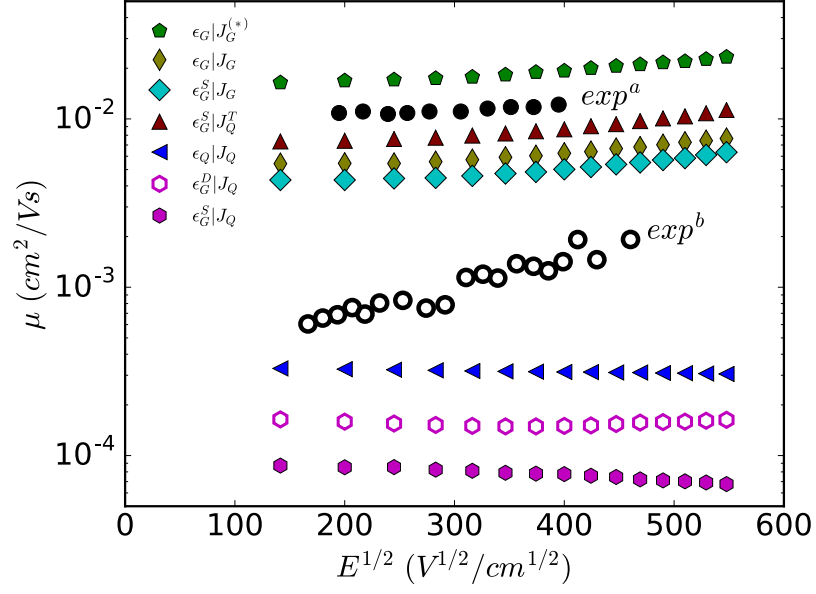
FIG. S11. Effect of simulation parameters on the mobility at 295 K. Filled and empty circles dots correspond to experimental time of flight measurements for references [18][(a)] and [16][(b)], respectively.